Electronic Supplementary Material (ESI) for Sustainable Energy & Fuels.
This journal is © The Royal Society of Chemistry 2024

Supplementary Information

Bifunctional Pt-Ir Nanoparticle Catalysts for Oxygen Reduction and Evolution Reactions: Investigating the Influence of Surface Composition on the Catalytic Properties

Lucinda Blanco-Redondo*[a], Yevheniia Lobko*[a], Kateřina Veltruská[a], Jaroslava Nováková[a], Michal Mazur[b], Alina Madalina Darabut[a], Tomáš Hrbek[a], Milan Dopita[c], Jakub Hraníček,[d] Yurii Yakovlev,[a] Iva Matolínová[a], Vladimír Matolín[a]

[a]Charles University, Faculty of Mathematics and Physics, Department of Surface and Plasma Science, V Holešovičkách 2, 180 00 Prague 8, Czech Republic.
[b]Charles University, Faculty of Science, Department of Physical and Macromolecular Chemistry, Hlavova 8, 12800 Prague 2, Czech Republic.
[c]Charles University, Faculty of Mathematics and Physics, Department of Condensed Matter Physics, Ke Karlovu 5, 121 16 Prague 2, Czech Republic.
[d] Charles University, Faculty of Science, Department of Analytical Chemistry, Hlavova 2030/8, 128 00 Prague 2, Czech Republic

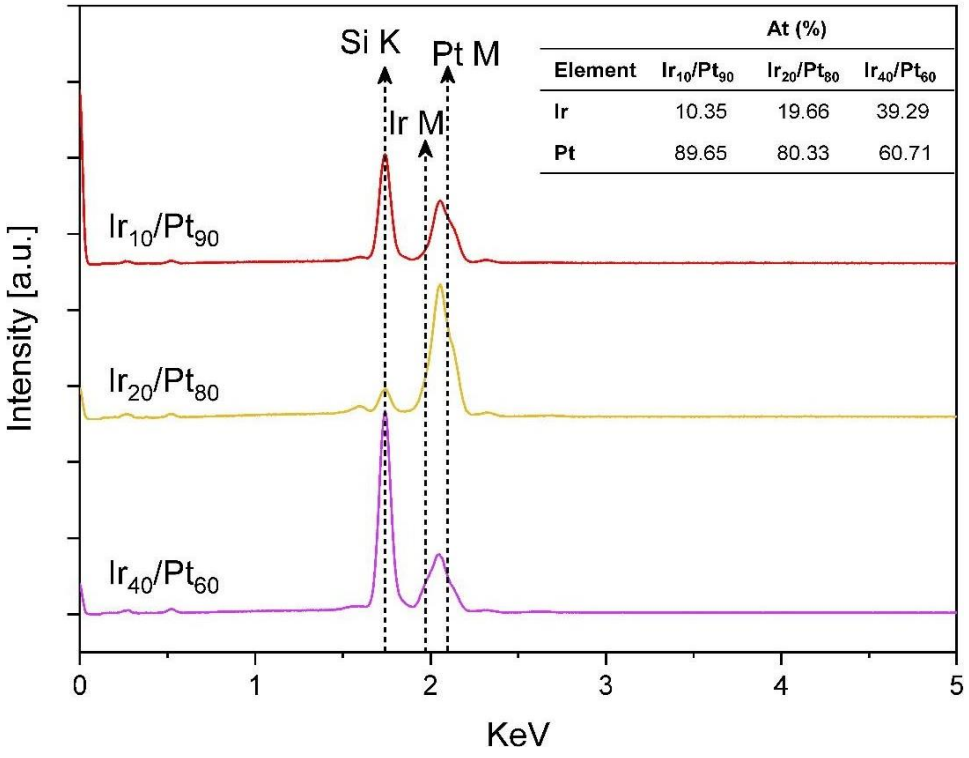

At (%)			
Element	Ir_{10}/Pt_{90}	Ir_{20}/Pt_{80}	Ir_{40}/Pt_{60}
Ir	10.35	19.66	39.29
Pt	89.65	80.33	60.71

Figure S1. EDX spectra of the nanoparticles on a silicon wafer.

USED EQUATIONS:

The CO surface area $ECSA_{CO}$ in cm^2 was determined using equation:

$$ECSA_{CO} = \frac{Q_{CO}}{monolayer\ of\ absorbed\ CO} \qquad (S\ 1)$$

*Corresponding authors.
E-mail address: yevheniia.lobko@mff.cuni.cz (Y. Lobko).

where Q_{CO} is the CO stripping charge and the monolayer of absorbed CO charge are 420 and 376 $\mu C \cdot s^{-1}$ for platinum and iridium, respectively.

The specific surface area (SA_{ORR}) and mass activity (MA_{ORR}) were obtained by normalization of j_k as follows:

$$SA_{ORR} = \frac{j_k}{ECSA_{Hupd} \cdot metal\ loading} \quad (S\ 2)$$

$$MA_{ORR} = \frac{j_k}{metal\ loading} \quad (S\ 3)$$

The number of electrons involved in the reactions and the percentage of H_2O_2 produced are calculated from equations S5 and S6, respectively.

$$n = 4 \cdot \frac{I_d}{I_d + I_r/N} \quad (S\ 4)$$

$$\%HO_2^- = 200 \cdot \frac{I_r/N}{I_d + I_r/N} \quad (S\ 5)$$

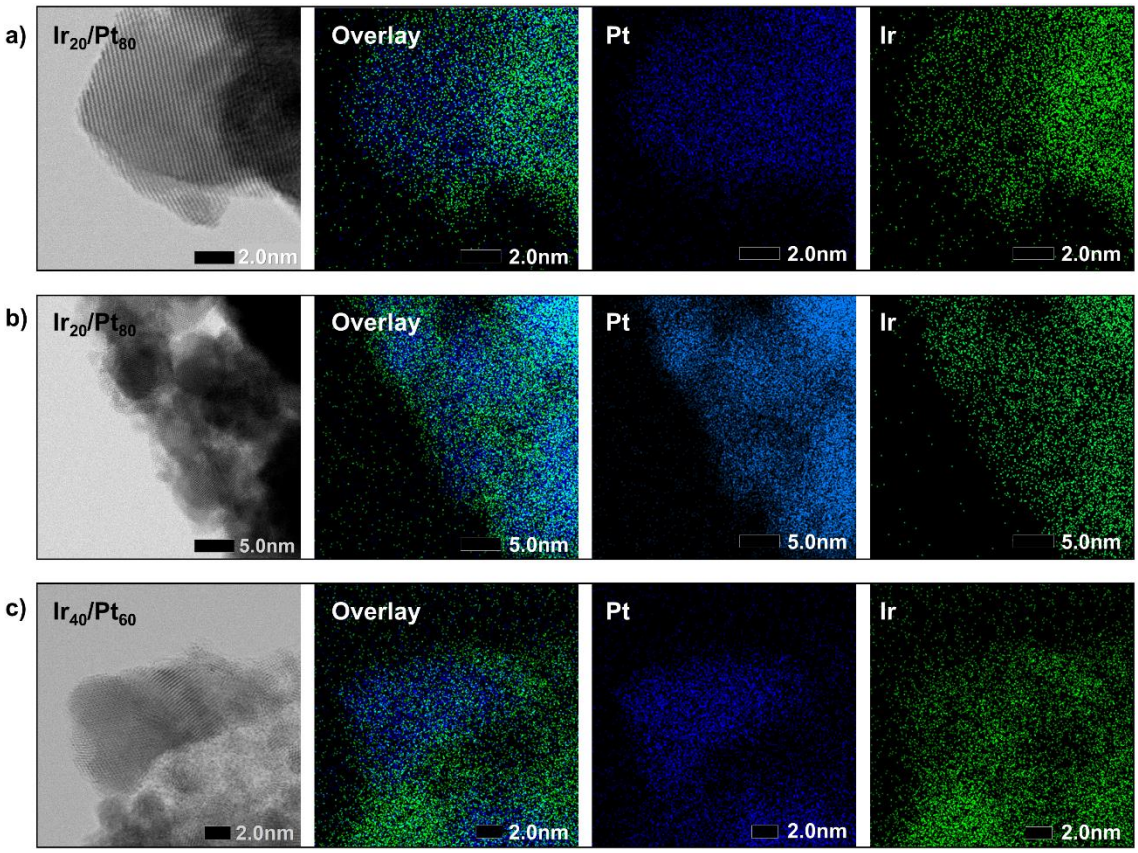

Figure S2. STEM-EDX elemental mapping images of Ir_{20}/Pt_{80} (a, b), and Ir_{40}/Pt_{60} (c) before electrochemical activation.

*Corresponding authors.
E-mail address: yevheniia.lobko@mff.cuni.cz (Y. Lobko).

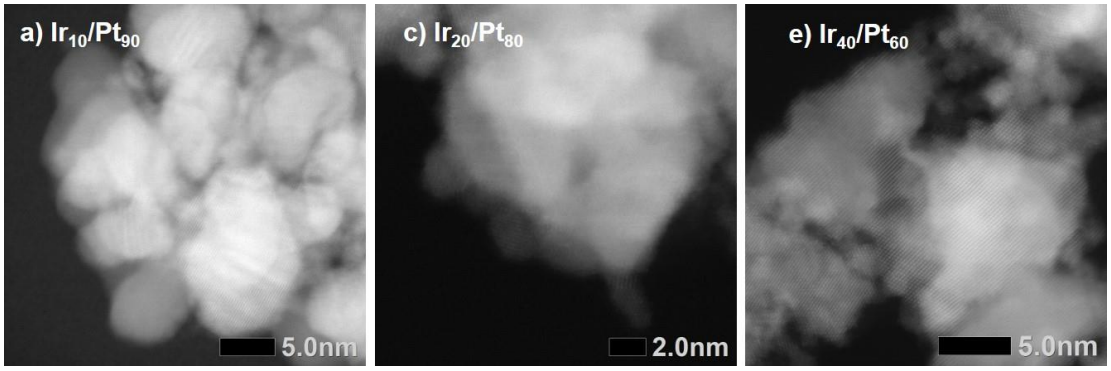

Figure S3. HAADF-STEM images of $Ir_{10}Pt_{90}$ (a), $Ir_{20}Pt_{80}$ (b), and $Ir_{40}Pt_{60}$ (c) before electrochemical activation.

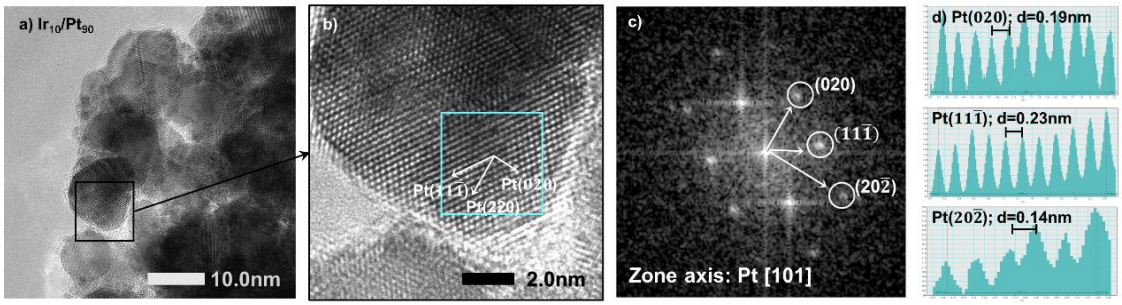

Figure S4. HR-TEM images (a, b), FTT pattern (c), and line intensity profiles (d) of Ir_{10}/Pt_{90}.

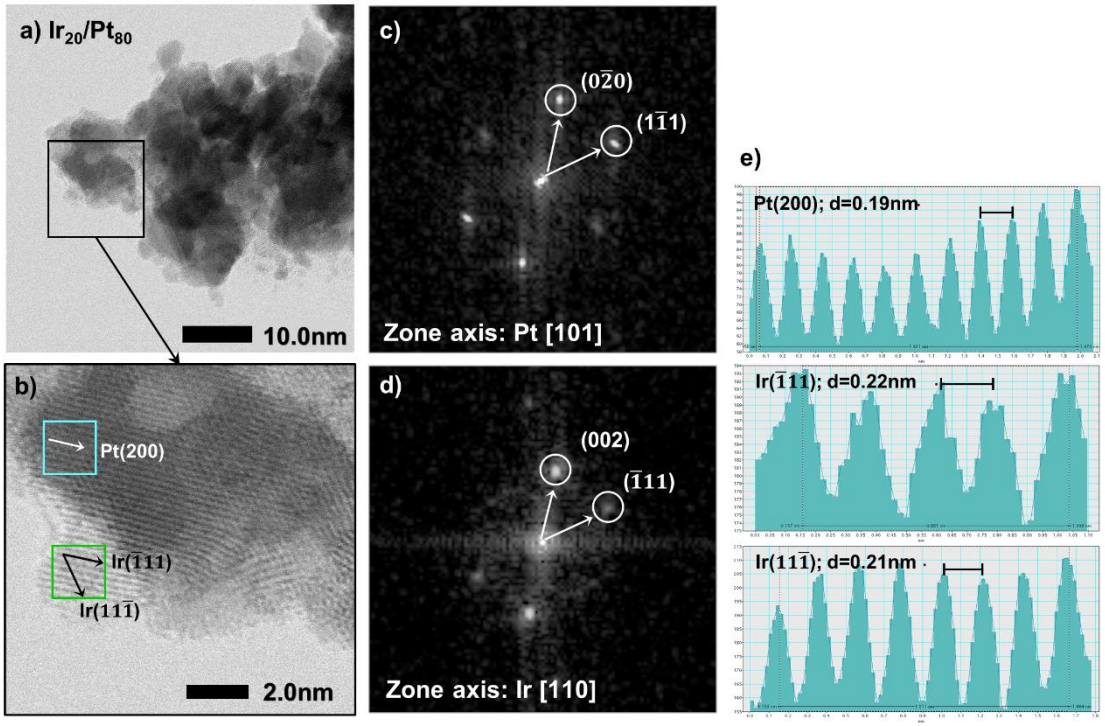

Figure S5. HR-TEM images (a, b), FTT pattern (c, d), and line intensity profiles (e) of Ir_{20}/Pt_{80}.

*Corresponding authors.
E-mail address: yevheniia.lobko@mff.cuni.cz (Y. Lobko).

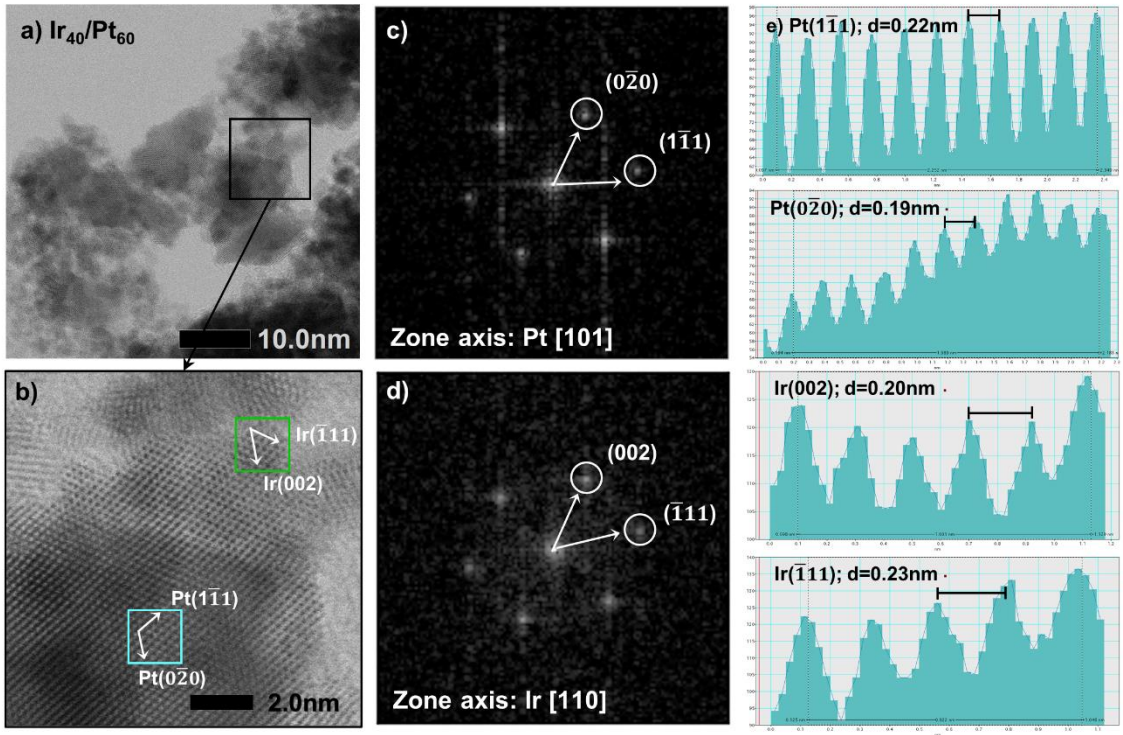

Figure S6. HR-TEM images (a, b), FTT pattern (c, d), and line intensity profiles (e) of Ir_{40}/Pt_{60}.

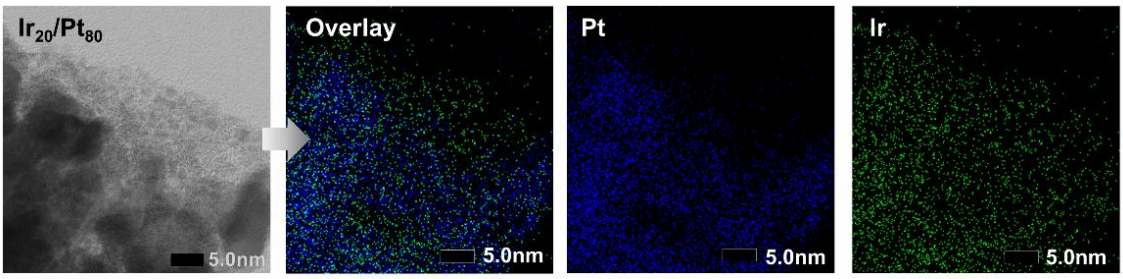

Figure S7. STEM micrograph and EDX elemental mapping of Ir_{20}/Pt_{80} after electrochemical activation.

Table S1. XRD parameters: lattice constant, mean crystallite size, and microstrain.

Sample	Lattice constant, a [Å]	error a [Å]	Mean crystallite size, D [nm]	error D [nm]	Microstrain, e [%]
Pt black	3.9181	0.00023	8.71	0.11	0.55
Ir_{10}/Pt_{90}	3.9145	0.00048	8.13	0.12	0.55
Ir_{20}/Pt_{80}	3.9139	0.00048	7.57	0.11	0.57
Ir_{40}/Pt_{60}	3.9123	0.00058	5.88	0.13	0.57
Ir black	3.8415	0.00071	2.91	0.13	0.65

*Corresponding authors.
E-mail address: yevheniia.lobko@mff.cuni.cz (Y. Lobko).

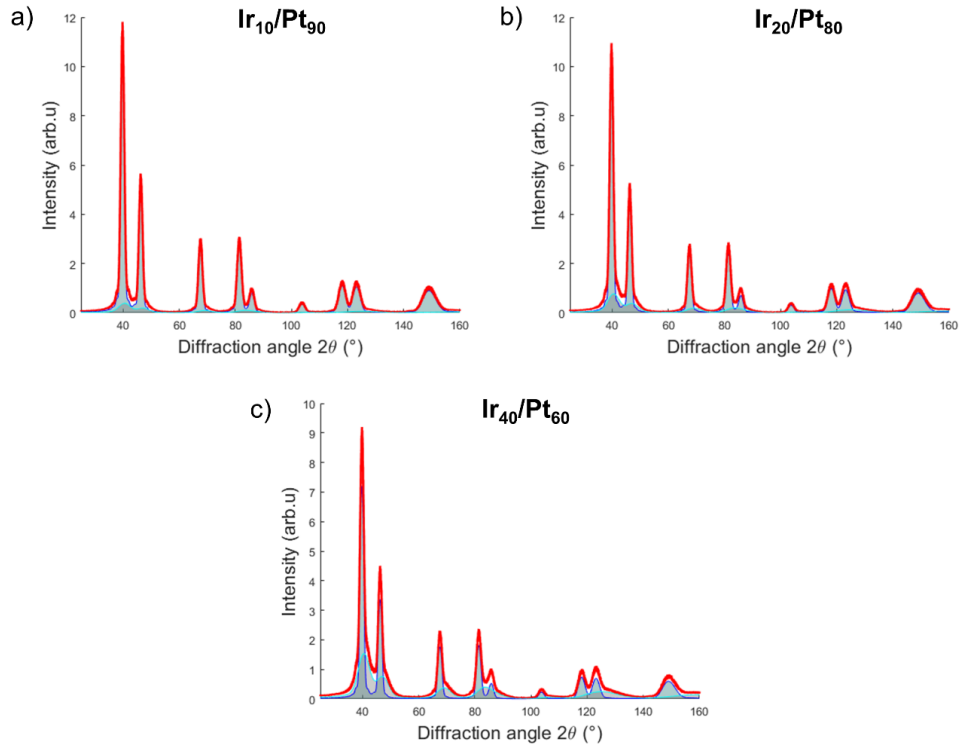

Figure S8. Simulation of the XRD patterns for Ir_{10}/Pt_{90} (a), Ir_{20}/Pt_{80} (b), and Ir_{40}/Pt_{60} (c) NPs. The blue curves are the Pt patterns, the cyan curves are the Ir patterns, and the red curve is the sum of both contributions. In the simulations done using the generalized Debye scattering equation, we considered the crystallite size broadening effect only, not the microstrain contribution.

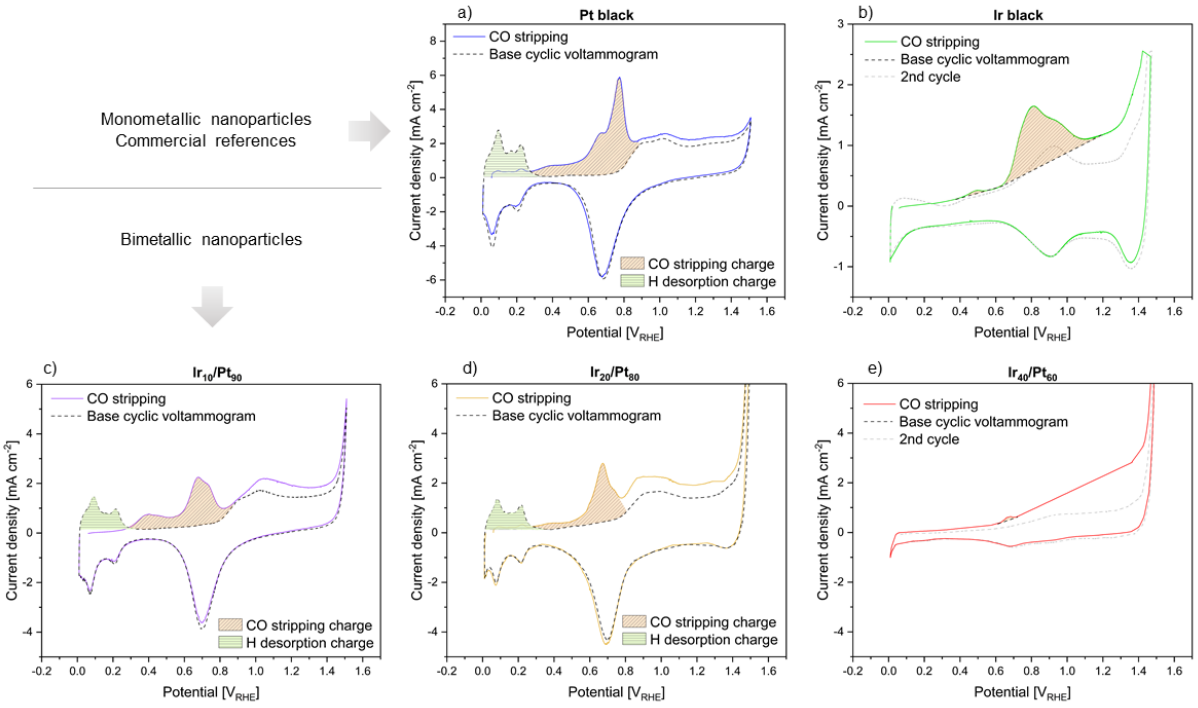

Figure S9. CO voltammetry curves of Pt black (a), Ir black (b), Ir_{10}/Pt_{90} (c), Ir_{20}/Pt_{80} (d), and Ir_{40}/Pt_{60} (e).

*Corresponding authors.
E-mail address: yevheniia.lobko@mff.cuni.cz (Y. Lobko).

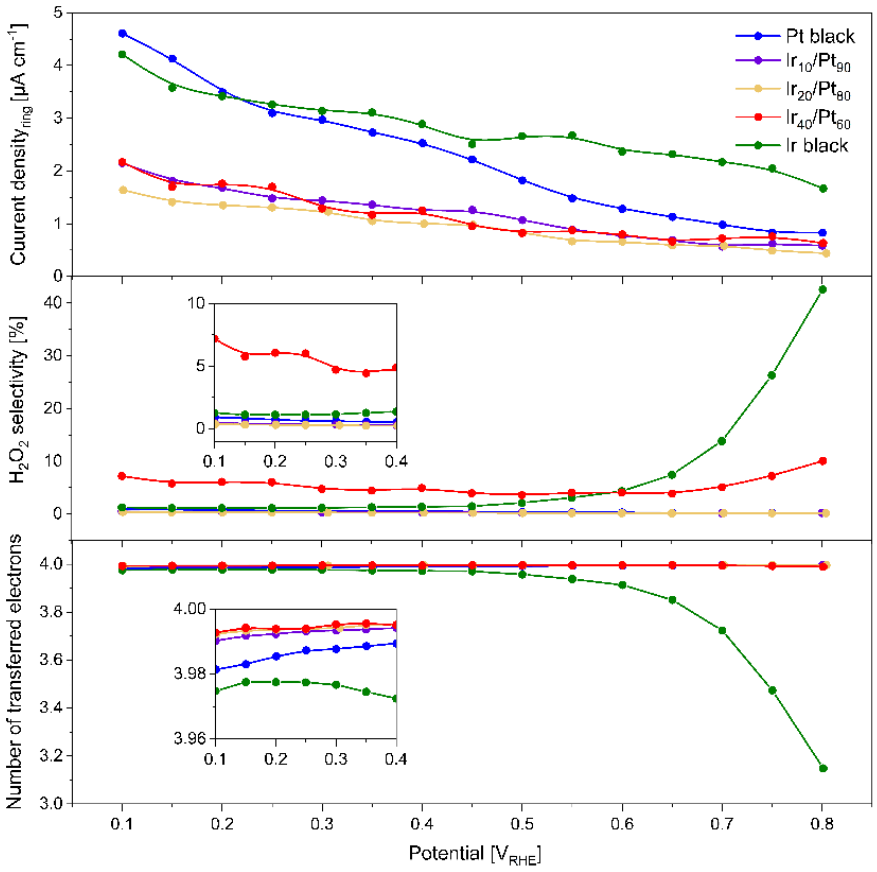

Figure S10. Chronoamperometry of the detected H_2O_2 current on the ring electrode (a). Calculated electron transfer number (b) and H_2O_2 selectivity (c) during potential sweep.

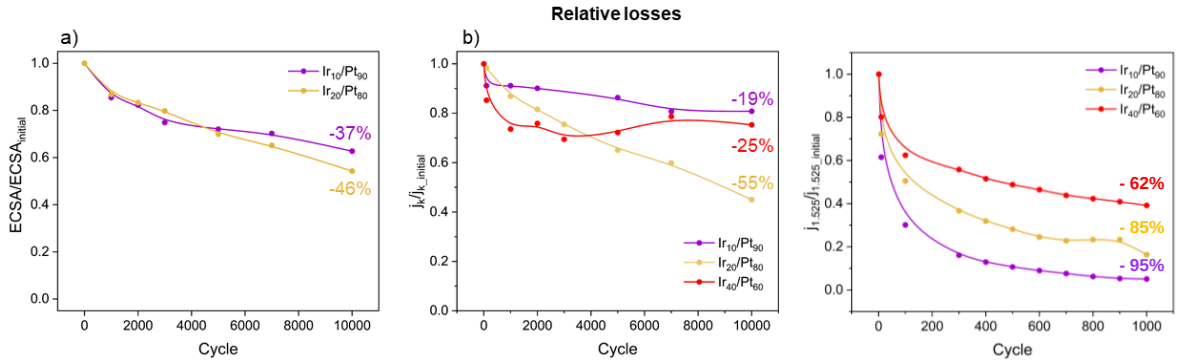

Figure S11. Accelerated stress test: Relative losses in ECSA (a), ORR activity (b), OER activity (c).

*Corresponding authors.
E-mail address: yevheniia.lobko@mff.cuni.cz (Y. Lobko).